

Bulletin of the Geological Society of Greece

Vol. 53, 2018



The Walls of Eupalinos Aqueduct, Samos Island, Greece. Description, Pathology and Proposed Restoration Measures

Angistalis Georgios
Dounias Georgios
Tsokas Grigorios

Egnatia Odos S.A.
Edafos S.A
Aristotle University of
Thessaloniki
Costas Zambas and
Associates

Zambas Costas

<http://dx.doi.org/10.12681/bgsg.18710>

Copyright © 2018 Georgios Angistalis



To cite this article:

Angistalis, G., Dounias, G., Tsokas, G., & Zambas, C. (2018). The Walls of Eupalinos Aqueduct, Samos Island, Greece. Description, Pathology and Proposed Restoration Measures. *Bulletin of the Geological Society of Greece*, 53(1), 193-228. doi:<http://dx.doi.org/10.12681/bgsg.18710>

*Research Paper*

Correspondence to:
Georgios Angistalis
gaggis@egnatia.gr

DOI number:
<http://dx.doi.org/10.12681/bgsg.18710>

Keywords:
*Eupalinos, Aqueduct,
Walls, Pathology,
Investigation,
Restoration*

Citation:
Angistalis Georgios,
Dounias Georgios, Tsokas
Grigorios, Zambas Costas
(2018), The Walls of
Eupalinos Aqueduct,
Samos Island, Greece.
Description, Pathology and
Proposed Restoration
Measures. Bulletin
Geological Society of
Greece, 53, 193-228.

Publication History:
Received: 04/10/2018
Accepted: 14/11/2018
Accepted article online:
14/11/2018

The Editor wishes to thank
Prof. M. Stamatakis and
Ms Erietta Vlachou for
editorial assistance.

©2018. The Author
This is an open access
article under the
terms of the Creative
Commons Attribution
License, which permits
use, distribution and
reproduction in any
medium, provided the
original work is
properly cited

THE WALLS OF EUPALINOS AQUEDUCT, SAMOS ISLAND, GREECE. DESCRIPTION, PATHOLOGY AND PROPOSED RESTORATION MEASURES

Georgios Angistalis¹, Georgios Dounias², Grigorios Tsokas³, Costas Zambas⁴

¹Egnatia Odos S.A, gaggis@egnatia.gr

²Edafos S.A., gdounias@edafos.gr

³Aristotle University of Thessaloniki, gtsokas@geo.auth.gr

⁴Costas Zambas and Associates, c-zambas@hol.gr

Abstract

The Aqueduct of Eupalinos was built in the mid-sixth century B.C, on the island of Samos that lies in the archipelago of the north Aegean Sea. Herodotus (481-425 B.C.) was the first historian to refer to the monument. He names Eupalinos, son of Naustrophus, born in the city of Megara as the engineer responsible for the design and construction of this ancient project. He also describes the method of construction that makes this monument unique: "...One is a tunnel, under a hill one hundred and fifty fathoms high, carried entirely through the base of the hill; its excavation started from two portals (αρζάμενον, ἀμφίστομον) ...". Egnatia Odos S.A². in cooperation with the Prefecture of Samos and the Ministry of Culture initiated a multi-discipline design study to protect and restore the monument. The designs included surveying works, geological and geophysical investigations, as well as geotechnical, structural and architectural works. The main component of the aqueduct is the 1036 m long tunnel described by Herodotus. For a length of 165 m the tunnel is protected by dry masonry walls and vaults of remarkable quality, built in the Archaic era. For a length of 63 m it is protected by mortared masonry walls and vaults, built in the Roman-era. These walls at some locations have suffered significant deformation, due to ground pressures, and have partially failed. In order to restore the damaged sections of the wall, its structure was investigated with the use of ground penetrating radar (GPR)

and Electrical Resistivity Tomography (ERT). These methods indicated the thickness of the wall and to some extent the width of the excavation behind it. The space between the dry masonry of the Archaic wall and the excavation perimeter is backfilled with well stacked partially hewn stones. GPR seems to accurately determine the thickness of the massive building stones (20 to 40 cm thick) that form the wall's sides. ET seems to accurately determine the interface between the excavation perimeter and the backfill. The thickness of the backfill and the wall was found to range from 60 cm to 200 cm. This most likely suggests that at the protected sections the tunnel excavation suffered significant and systematic ground collapses. This is because the derived tunnel excavation dimensions at that point are much larger than the ones of the unprotected tunnel. The latter combined with the high ground water inflows now present, in the area and the identified poor ground conditions, could justify the decision of Eupalinos to protect the tunnel's excavation perimeter with the dry masonry walls. Other geophysical and geological investigations identified significant fault zones that cross the tunnel at the previously mentioned locations, where the assumed ground collapses were observed.

A simplified deformation analysis that was carried out using finite element modelling shows that the deformation and the observed wall failures can be roughly explained by assuming poor ground conditions around the tunnel. The protection/restoration measures that were dimensioned for the Archaic type wall include: a) a staged, stone by stone, dismantling of the vaults and partially of the wall, b) supporting the ground behind them with stainless steel rock bolts, steel sets and a concrete mantle, and c) rebuilding the whole at its original "pre-deformed" position. These measures (steel sets, concrete mantle and rock bolts) aim in undertaking the full ground load so that the wall, when rebuilt, will be practically unloaded. Due to the different loading conditions and ground failure mode, the restoration measures designed for the Roman-era wall, aim to remove the rock (load) that fell on the roof arch, to prevent further rock falls and to strengthen the mortared masonry with neutral grouts.

Keywords: Eupalinos, Aqueduct, Walls, Pathology, Investigation, Restoration

Περίληψη

Το Ευπαλίνειο Υδραγωγείο κατασκευάστηκε στα μέσα του 6^{ου} π.Χ. αιώνα στην Σάμο στο αρχιπέλαγο το Βορείου Αιγαίου. Ο Ηρόδοτος (481-425 π.Χ.) είναι ο πρώτος ιστορικός που αναφέρεται στο μνημείο. Αναφέρει τον Ευπαλίνο, γιο του Ναυστρόφου από τα Μέγαρα ως τον υπεύθυνο μηχανικό για την μελέτη και την κατασκευή του μνημείου. Επίσης περιγράφει και την μέθοδο κατασκευής που το κάνει μοναδικό: «...κατάφεραν να διανοίξουνε μία σήραγγα από δύο στόμια (αρζάμενον, αμφίστομον), στην βάση ενός βουνού ύψους 150 μέτρων». Η Εγνατία Οδός Α.Ε. σε συνεργασία με την Νομαρχία της Σάμου και το Υπουργείο Πολιτισμού ξεκίνησαν την εκπόνηση μίας πολυθεματικής μελέτης με σκοπό την προστασία και την αποκατάσταση του μνημείου. Η μελέτη συμπεριλάμβανε τοπογραφικές εργασίες, γεωλογικές και γεωφυσικές έρευνες όπως και στατικές, γεωτεχνικές και αρχιτεκτονικές εργασίες. Το βασικό τμήμα του υδραγωγείου είναι η σήραγγα μήκους 1036 μ που περιγράφεται από τον Ηρόδοτο. Για μήκος 165 μ η σήραγγα είναι επενδυμένη από λιθοδομή, εξαιρετικής ποιότητας κατασκευής, που χρονολογείται στην Αρχαϊκή εποχή. Επίσης, για μήκος 63 μ είναι επενδυμένη από λιθοδομή κατασκευασμένη από πλίνθους συγκολλημένους με κονίαμα. Αυτή η λιθοδομή χρονολογείται στην Ρωμαϊκή εποχή. Αυτές οι επενδύσεις σε κάποιες θέσεις έχουν παραμορφωθεί εξαιτίας γεωστατικών πιέσεων και μερικώς έχουν αστοχήσει. Στα πλαίσια των μελετών αποκατάστασής τους έγιναν διερευνήσεις με GPR (Ground Penetration Radar) και ηλεκτρικές διασκοπήσεις ERT (Electrical Resistivity Tomograph). Με τις μεθόδους αυτές διερευνήθηκε το πάχος της επένδυσης και σε κάποιο βαθμό και το πλάτος της εκσκαφής από πίσω τους. Ο χώρος μεταξύ της Αρχαϊκής επένδυσης και της περιμέτρου της εκσκαφής είναι πληρωμένος με καλά στοιβαγμένους λίθους μερικώς επεξεργασμένους. Η μέθοδος GPR φαίνεται να εκτιμά με καλή ακρίβεια το πάχος των δομικών λίθων που συνιστούν τις παρειές της επένδυσης (20 εκ. έως 40 εκ). Η μέθοδος ERT φαίνεται να εκτιμά με καλή ακρίβεια την θέση της περιμέτρου της υπόγειας εκσκαφής ή αλλιώς την διεπιφάνεια της εκσκαφής με το υλικό πλήρωσης. Το πάχος της πλήρωσης συν αυτό της επένδυσης βρέθηκε να κυμαίνεται από 60 εκ έως 200 εκ.

Κατά πάσα πιθανότητα αυτό σημαίνει πως στα προστατευμένα τμήματα της σήραγγας επισυνέβησαν σημαντικές και συστηματικές καταρρεύσεις του εδάφους. Και αυτό γιατί οι προκύπτουσες διαστάσεις της υπόγειας εκσκαφής στις περιοχές αυτές, προκύπτουν σημαντικά μεγαλύτερες από τις αντίστοιχες στα μη προστατευμένα τμήματα της σήραγγας. Αυτή η παρατήρηση σε συνδυασμό με την μεγάλη υδροφορία και τα διαπιστωμένα μαλακά εδάφη στα ίδια τμήματα, θα μπορούσε να εξηγήσει την απόφαση του Ευπαλίνου να προστατεύσει την περίμετρο της υπόγειας εκσκαφής με λιθοδομή. Επιπρόσθετα άλλες γεωφυσικές και γεωλογικές έρευνες εντόπισαν ζώνες ρηγμάτων που τέμνουν την σήραγγα στις προαναφερθείσες θέσεις, εκεί δηλαδή που πιθανολογούνται εδαφικές αστοχίες. Μία απλοποιημένη ανάλυση με την μέθοδο των πεπερασμένων στοιχείων ερμηνεύει τις παρατηρούμενες παραμορφώσεις της επένδυσης υποθέτοντας την ύπαρξη μαλακού εδάφους στην περίμετρο της σήραγγας.

Τα μέτρα προστασίας/αποκατάστασης που διαστασιολογήθηκαν για την Αρχαϊκή επένδυση περιλαμβάνουν: α) αποσυναρμολόγηση της οροφής λίθο προς λίθο και μερικώς, των παρειών της επένδυσης, β) υποστήριξη του εδάφους με ανοξείδωτα αγκύρια, πλαίσια και μανδύα από σκυρόδεμα, και γ) ανακατασκευή της επένδυσης στην αρχική της γεωμετρία, δηλαδή στην γεωμετρία που είχε πριν παραμορφωθεί. Τα μέτρα αυτά (τα μεταλλικά πλαίσια, τα αγκύρια και μανδύας του σκυροδέματος) θα παραλάβουν το σύνολο των γεωστατικών φορτίων έτσι ώστε η επένδυση να είναι στην τελική της κατάσταση αφόρτιστη. Όσον αφορά στην Ρωμαϊκή επένδυση, λόγω των διαφορετικών καταστάσεων φόρτισής της και του τύπου αστοχίας του εδάφους εκεί, τα μέτρα αποκατάστασης περιλαμβάνουν την απομάκρυνση του αστοχήσαντος εδάφους πάνω από τον θόλο της πρώτης, την αποσόβηση νέων καταπτώσεων και την ενίσχυση της λιθοδομής με αδρανή ενέματα.

Λέξεις κλειδιά: Ευπαλίνος, Υδραγωγείο, Επένδυση, Παθολογία, Έρευνα, Αποκατάσταση

1.Introduction

The Aqueduct of Eupalinos has a total length of over 2,5 km, involving a bored tunnel 1036 m long, ~1.8 m x 1,8 m wide under a 170 m overburden of mount Kastro. Part of the aqueduct was constructed as an open trench ~60 cm wide and of a variable height (in the order of some meters). The trench is covered with big orthogonal hewn stones or an arched shaped roof. Another part of it was constructed with the use of the “shaft and gallery” method, which involves the construction of vertical shafts interconnected underground. The most interesting part of the aqueduct is the main 1036 m long bored tunnel that “hosts” the canal (or trench) and the water conveying ceramic pipeline. It comprises two sections. The north section is 610 m long and the south section is 426 m long. The excavation works of these sections met under the apex of mount Kastro (Figure 1). For a length of approximately 165 m they are protected by an Archaic-era wall made out of dry masonry with very well hewn, stones. Big, slightly curved stones shape the triangular roof of the wall. For a length of 63 m, at the north bore the tunnel was subsequently protected by a Roman-era mortared rubble stone wall with an arched roof.

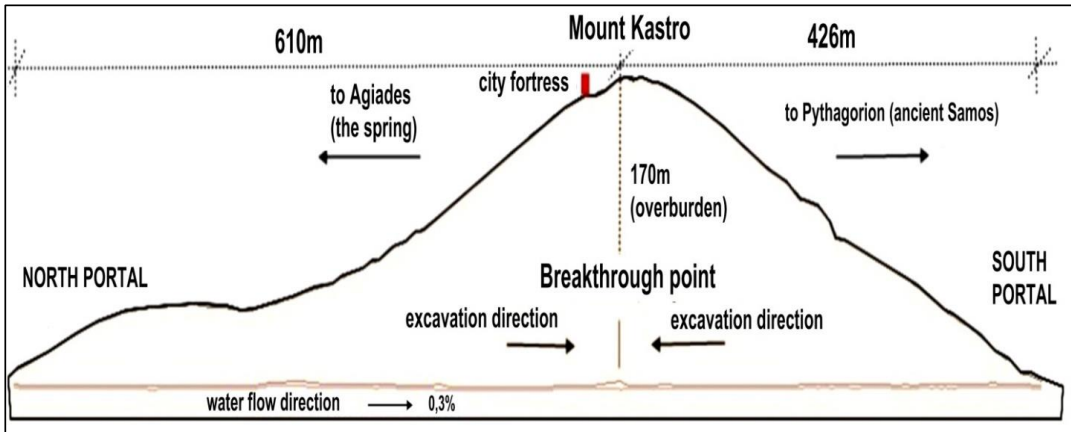


Fig. 1: Simplified longitudinal section of the tunnel (altitude of the walking levels: at north portal: +55,22, at south portal: +55,26, at the apex of mount Kastro: +225,00), (Angistalis and Kouroumli, 2013).

The monument is considered a milestone in tunnel engineering: the engineer breaks new ground and deviates from the classical, commonly used ones during that period, method of tunnel construction (the “shaft and gallery” method), by building a tunnel under a mountain, starting digging from two portals that were diametrically opposite. He used mathematics and geometry not only to align the excavations, but also to “manipulate” the alignment of the tunnel in order to avoid adverse geological

conditions. Mutatis mutandis, the basic principle behind the method of Eupalinos, was used again long after the Renaissance in Europe (early 18th century), and it is still in use in modern tunnelling.

The architectural and archaeological study of the monument has been compiled by Dr. Hermann Kienast³ of the German Archaeological Institute of Greece. The initiative person behind this study was Ulf Jantzen, the former director of the institute. The study comprises 213 pages of text, plus 41 pages of high quality photographs and drawings. The study covers among other issues such as the monument's inspection and discovery, the concept behind its design and construction, the subsequent interventions, design, construction and functionality of the ancient works, mathematics and geometry of the tunnel alignment, the ancient marking and aligning systems, the meeting point of excavations, geometrical design assumptions, geological conditions, etc. His study is the only work that thoroughly describes and explains the aqueduct of Eupalinos in the most detailed way. An extensive abstract of this study can be found in a widely available booklet published by the Ministry of Culture (available in English⁴).

2. The materials of the walls and their pathology

2.1 Brief description of the walls

Almost 238 m of the main 1036 m long tunnel were lined (protected). The 165 m of it were lined during or immediately after the completion of the excavation works. At the north tunnel section, the Archaic tunnel starts at ch 0+064 (i.e. 64 m from the north tunnel entrance) and ends at ch 0+263. Figure 2 shows the start of the Archaic wall at ch. 0+064. Here the east side of the wall is founded on in-situ ground. The west side is founded on a hewn stone that bridges the trench. This trench hosts the water conveying ceramic pipe. For more than 200 m, the trench has been excavated as a mined gallery and it is also protected by walls forming a triangular roof. The pattern of the wall classifies it as belonging to the Archaic era. Most of this trench is now filled with sediment. Elsewhere, i.e. when the trench is located in the middle of the tunnel - both sides of the wall are founded on hewn stones that bridge the trench. The foundation stones are 40 cm high, 72 cm wide and 150 cm long. The wall's sides are ~1,25 m high and are made of similar stones (see also Stamatakis, 1990). The curved stones (20-30 cm wide, ~60 cm long) are placed on the top of the sides, forming the wall's triangular roof (~45 cm high). The clearance dimension of the passageway is

~70 cm wide and 1,70 m high. Further inside, the wall's sides are made of stones with completely different dimensions. They are 8 to 12 cm thick also non mortared; their edges have been so meticulously treated, placed and adjusted that practically all joints are in full contact. Therefore, the stability of the wall results from the high hewing quality of its building stones and their subsequent tight placement and fixing works.

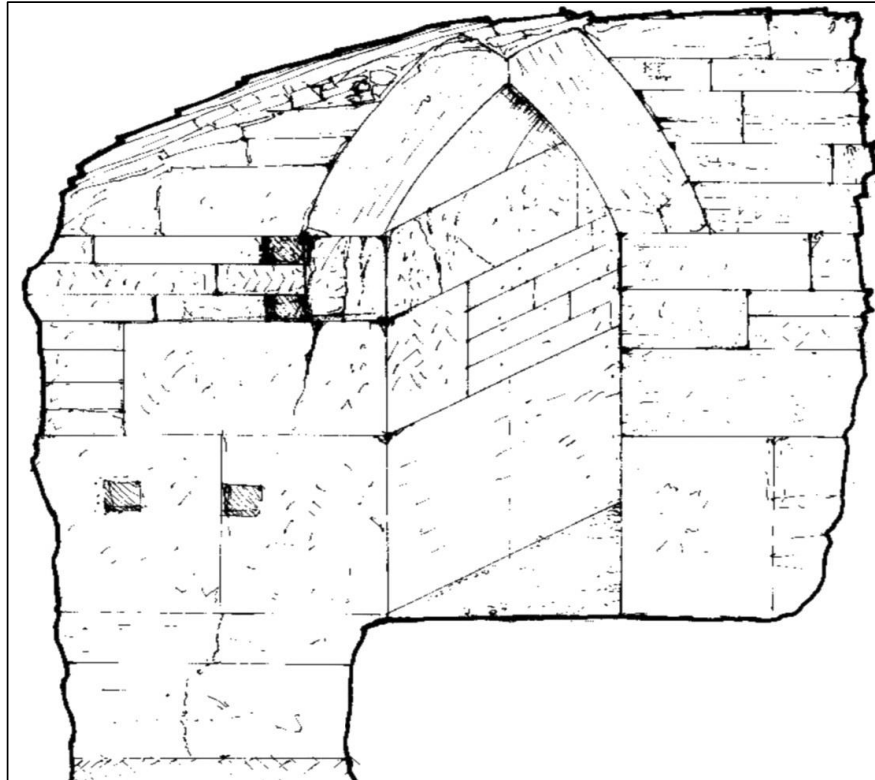


Fig. 2: View of the Archaic wall at ch 0+064.

An Archaic lining almost 13 m long was also constructed at the south tunnel portal. The side walls were not constructed with orthogonal stones, but with polygonal ones. The edges of these stones are well shaped and the contact joints between them are tight and completely closed. This lining was extended for another 7 m during the restoration works carried out in 1882⁵. In the middle of this tunnel section there is a vertical shaft, 80 cm by 60 cm in section, connecting the main tunnel with the ground surface. The shaft was reconstructed at the location of the ancient one, during the 1882 restoration works. The geometry of the side walls at the south portal is the same as that of the north tunnel bore.

The Roman lining at the north tunnel portal starts at ch. 0+014 and ends at ch 0+049 (35 m). It is made with a mortared masonry wall and an arched roof. The thickness of the mortared joints is ~3 cm, while the stone bricks of the vault are ~15 cm thick. The roof's arch, diligently constructed, has a height of 25 to 35 cm. Figure 3 shows a cross section of the lining's walls (at the north portal) built in the Roman era. A Roman-type wall also supports the sides and the roof of the trench. The horizontal clearance of the passageway is almost 0,60 m and the vertical is 1,60 m. Here, the orientation of the geological bedding is unfavorable for the stability of the tunnel's roof, which gradually collapsed on the vault.

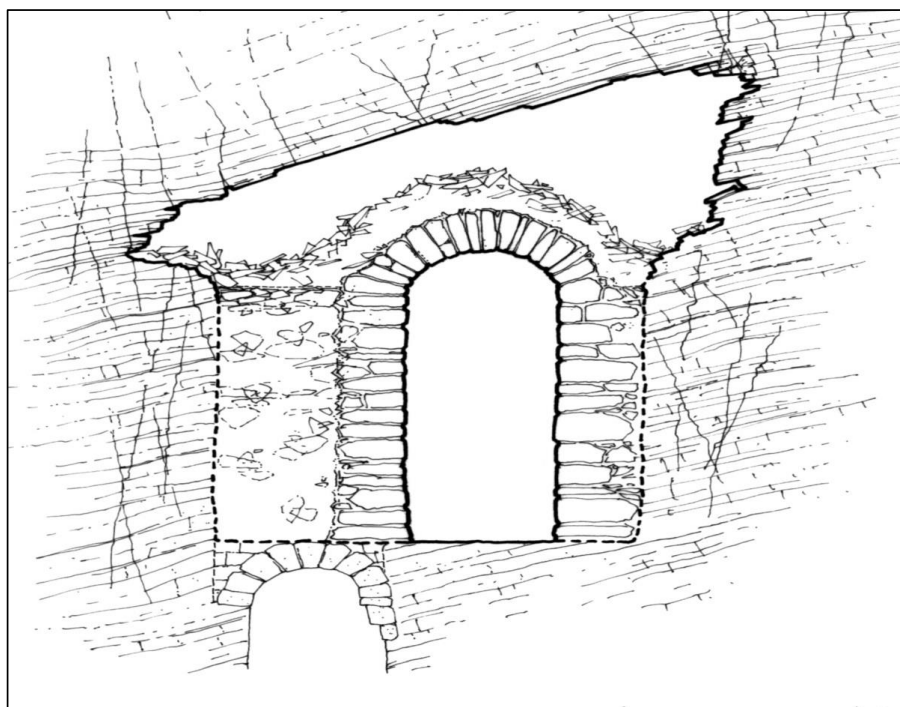


Fig. 3: Cross section of the main tunnel at the north portal showing the Roman type protective walls.

2.2 Pathology of the walls

Starting from the north tunnel portal, the Archaic wall is found to be deformed and fractured at seven locations. These wall damages are most likely stress induced due to the excessive ground loads. Chapter 3 examines in detail the most significant ones.

3. Methods and results of investigations at the dry masonry walls

3.1 Ground Penetration Radar (GPR) and Electrical Tomography (ERT) on the walls

A number of GPR and ERT tomographies were carried out on the masonry walls (Tsokas et al, 2014). The aim at these was to assess the thickness of the walls and image the space behind. The results of these methods are discussed in the paragraphs that follow. These concern locations of the walls of significant damages (e.g. fractured key stones, excessively deformed wall surfaces). At **ch 0+110**, the west tunnel wall was deformed to such an extent that no one could pass through. The west wall was partially reconstructed with mortared masonry during the early archaeological investigation (Figure 4). The reconstruction of the lining at this location offered the unique opportunity to see what lies behind it. The findings have been published by Kienast (1995).

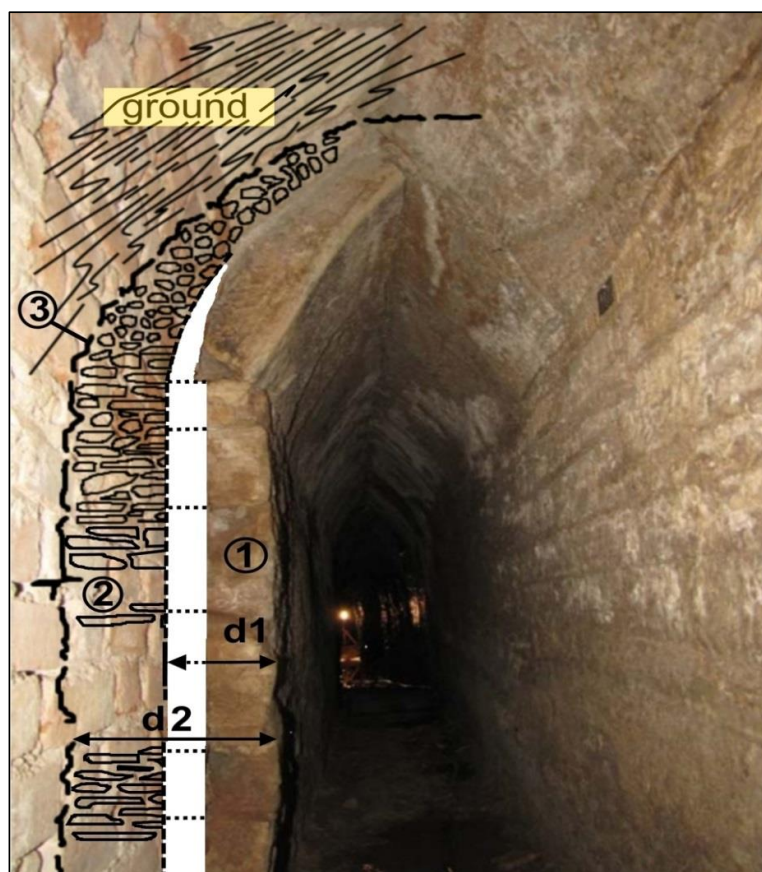


Fig. 4: Photograph of the reconstructed west sidewall (mortared masonry at the left hand side of the picture). The drawing overlay is a simplified representation of the space behind the walls.

The overlay in Figure 4 shows the structure of the tunnel behind the wall as this was revealed during the reconstruction works. Area 1 represents the wall. The dimension “d1” is the thickness of the hewn stones of the deformed wall. The most important finding from an engineering viewpoint has been the presence of backfill material in the space between the lining and the excavation (area 2). The backfill was made up of well-stacked but poorly worked hewn stones. The backfill material is extended upwards over the arched stones of the roof. This backfilling serve an important engineering purpose: to confine the excavation and eliminate the conditions which could lead to a ground collapse behind the lining. The dimension “d2” thickens “d1” plus the thickness of the backfill material. Line 3 shows the ground-backfill interface. For comparison purposes only, the previously mentioned basic dimensions of the tunnel are also shown in Figure 5, a cross section of the walls of the south tunnel portal.

The wall was investigated by means of ground penetration radar (GPR) and electrical resistivity tomography (ERT). The evaluation of the GPR results is shown in Figure 6. It is obvious that the GPR method predicts the wall – backfill interface or in other words the thickness “d1” of the wall’s hewn stones. The actual thickness of the wall “d1” is almost 25 cm (Figure 5). It is practically identical with the one derived from the interpretation of the GPR results, dimension “d1” at Figure 6.

On the other hand, the ERT method predicts (Figure 7) the ground – backfill interfaces or in other words the sum of the thickness of the wall’s hewn stones “d1” plus the thickness of the backfill material. The actual thickness “d2” is almost 60 cm (Figure 5). It is practically identical with the one derived from the interpretation of the ERT results, dimension “d2” at Figure 7. GPR signal loss (no rebound measured), at approximately **ch 0+100** is justified by the high-water content that is observed in this area.

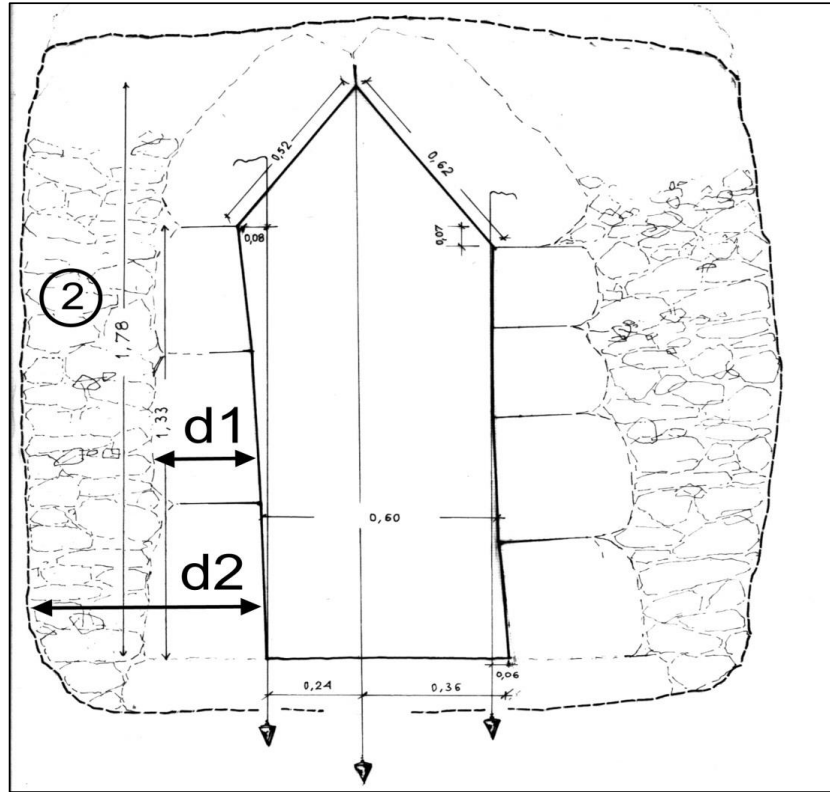


Fig. 5: Basic dimensions of the tunnel (walls at south tunnel portal). “d1” is the thickness of the hewn stones of the wall. “d2” is the sum of the thickness “d1” plus the thickness of the backfill material (area 2).

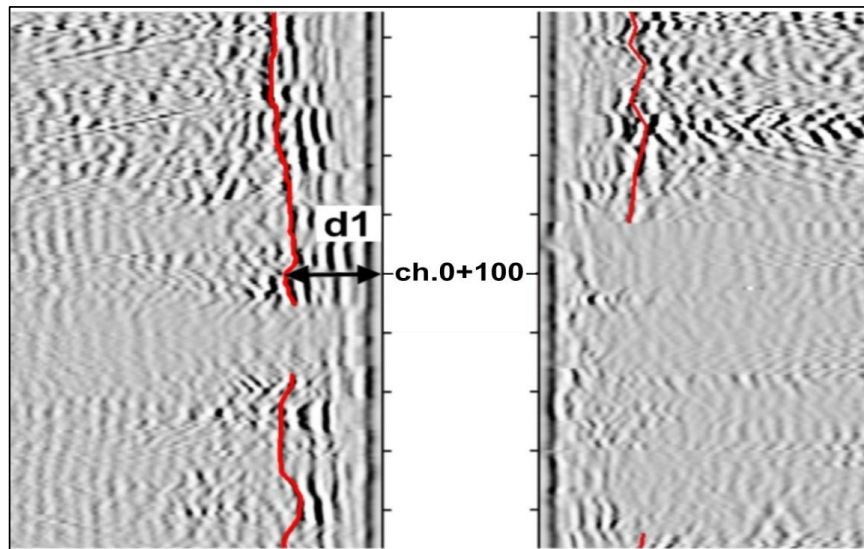


Fig. 6: Results of ground penetration at ch. 0+100.

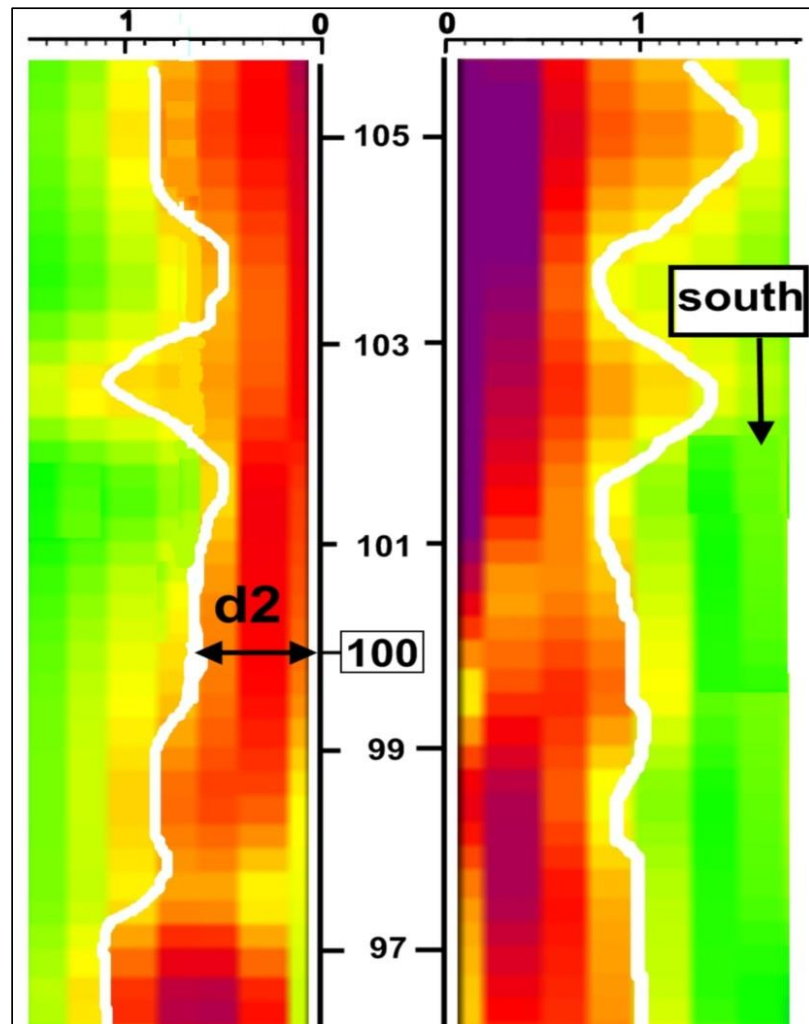


Fig. 7: Electrical resistivity results at ch. 0+100. High resistivity boundaries (white lines) match with the ground – backfill interface boundary.

Ch **0+064** is the starting point of the Archaic lining. At this point the lining suffers a minor but interesting damage: A few pieces/flakes have been detached from the front surface of the roof's arch stone i.e. at points 2 and 3 of Figure 8 and from its supportive stone i.e. at point 1 of Figure 8.

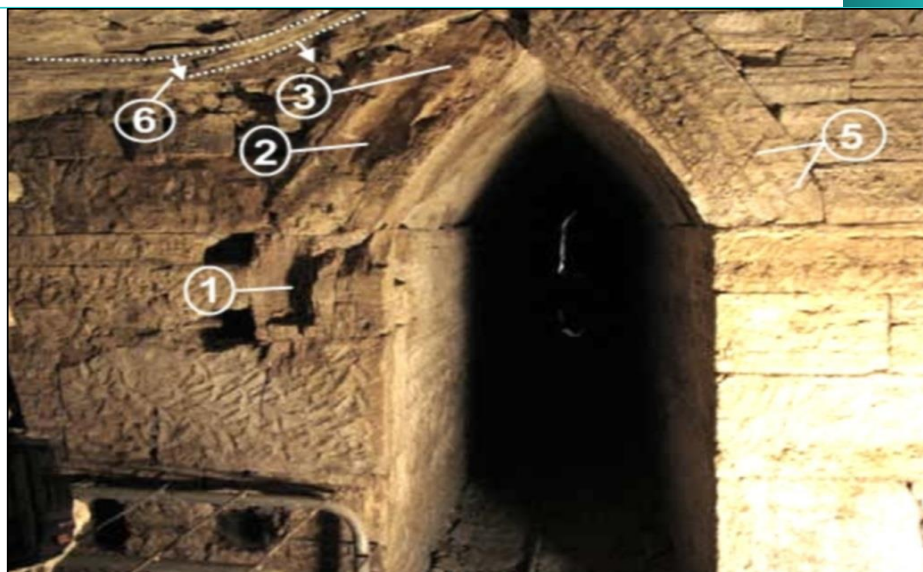


Fig. 8: Flakes detached from the front surface of the roof arch stones at points 1, 2 and 3. Two new cracks have been identified in the right roof slab at point 5. Point 6 shows the direction of the foliation/schistosity of the ground. The shot was taken in 2008.

The flake at the point no 3 in Figure 8 has been detached later than 1974. The two cracks at the right roof slab have also been formed after year 1974. Both the flake detachment and the cracks, were determined to have occurred after 1974 following comparison of a 1974 picture (DAI 74-2202 in Kienast, 1995) with a current one (2008).

Such an evidence found at a 2,6 thousand -year old monument can be considered as very rare. The spalling observed shows that the surrounding ground still stresses the masonry wall. In general it is also obvious that the west side of the wall is more distressed.

The thickness of the wall that starts from chainage **0+064** and further inside has been investigated by means of ground penetration radar (GPR) and electrical resistivity tomography (ERT). Figure 9 shows the basic dimensions “d1” and “d2”. Blue and red dots show the levels of the GPR and ERT scan lines.

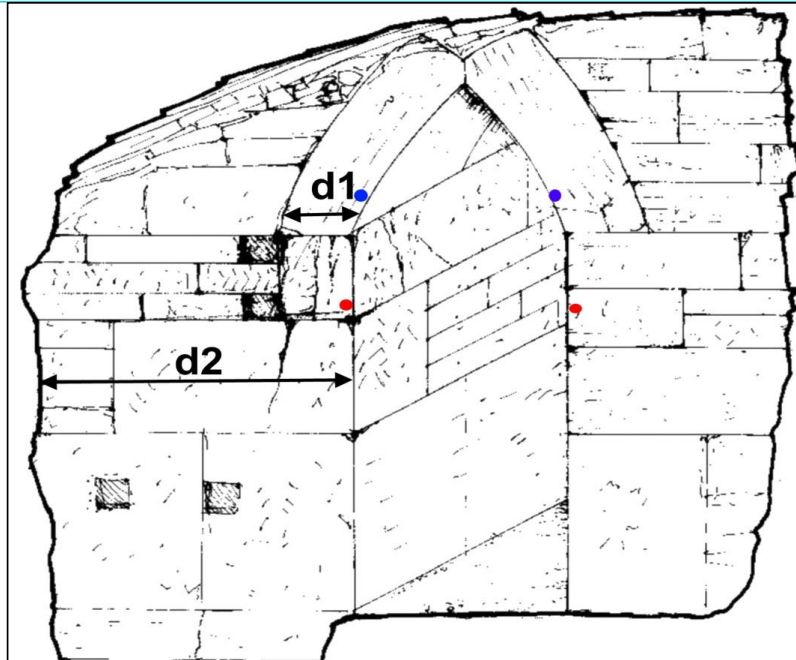


Fig. 9: Sketch of the tunnel wall of ch. 0+064. Blue and red dots show the levels of the GPR and ET scan lines.

Figures 10 and 11 show the results of the GPR. Figure 12 shows the ERT result at the west sidewall of the lining (at the level of the point). The comparison of the GPR results shows again that this method practically predicts the thickness of the solid hewn stones of the walls (backfill-wall interface).

The ERT method on the other hand estimates well the dimensions of the excavation profile (backfill-ground interface). An area with very low resistivity (blue area) at ch **0+070** has also been evaluated as an area with high water content. Dripping water is observed in this location.

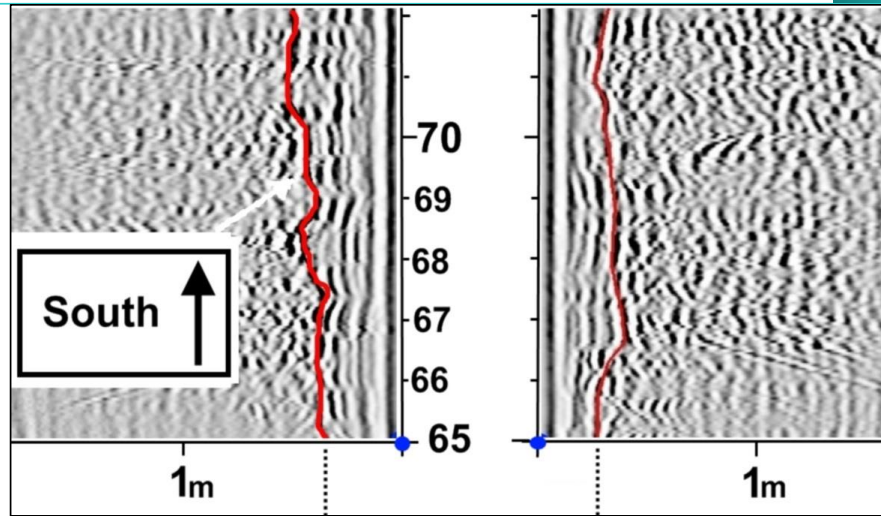


Fig. 10: Results of ground penetration radar at ch 0+64 at the level of the blue point. The graph shows the results from a 6-7 m long section of the tunnel’s lining to the South (from ch 0+064 to 0+072). The red line shows the thickness of the wall’s hewn stones.

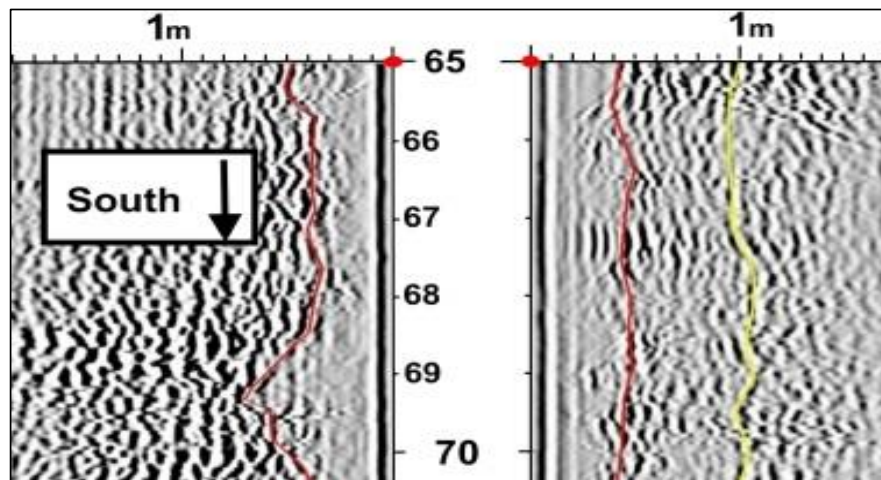


Fig. 11: Results of ground penetration radar at ch 0+63,9. The yellow line is most probably a significant joint or a fault running parallel to the tunnel.

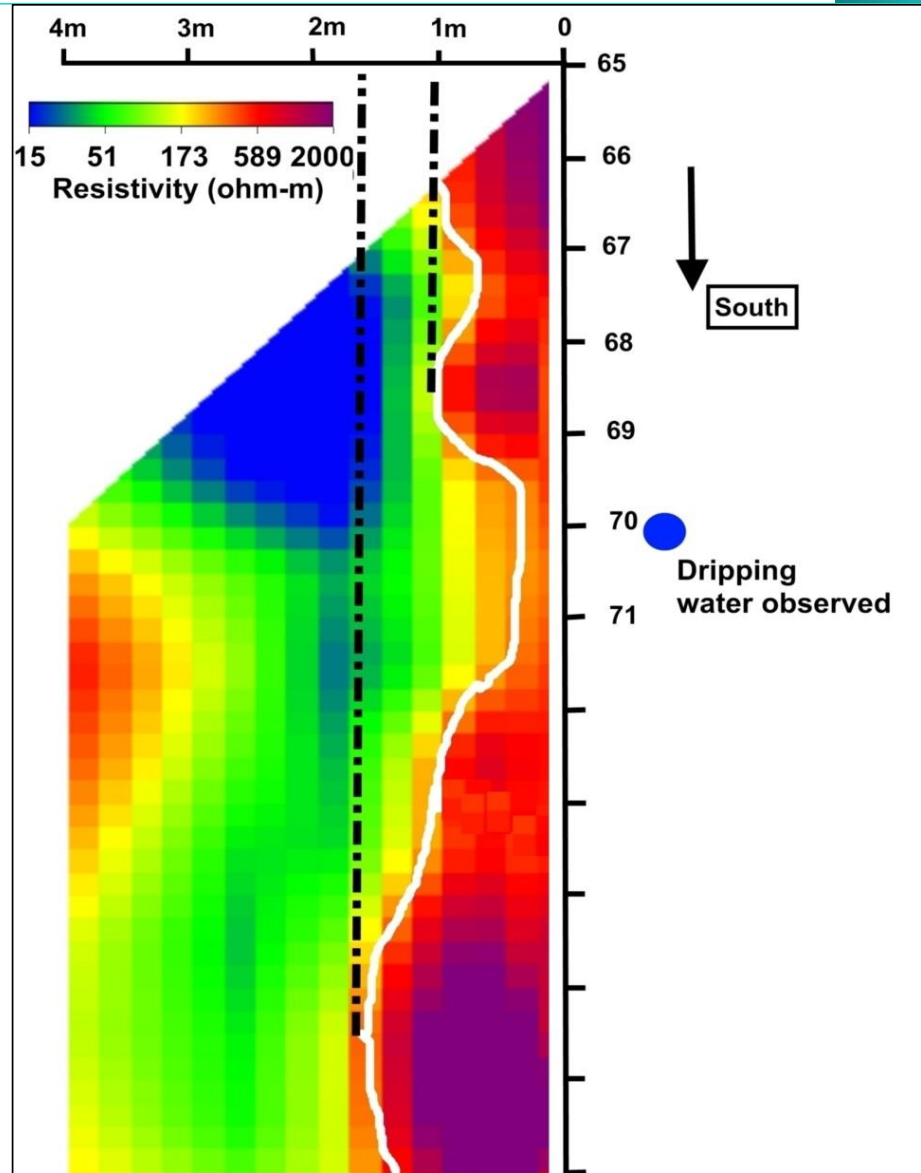


Fig. 12: Results of electrical resistivity tomography near ch 0+64 at the west sidewall of the lining. The white line represents the ground-backfill interface. The line that represents the interface is very uneven most likely due to the ground collapses that occurred during the tunnel drive.

From **ch 0+130** to **ch 0+136** the wall is highly deformed and the arched stones of the roof are displaced and fractured (Figure 13).



Fig. 13: The tunnel at ch. 0+130 with dislocated roof stones.

Figure 14 shows the GPR results and Figures 15 and 16 the ERT results. Electrical resistivity tomography has been used along four lines of the wall (two at either side). The lower ones were at 0,6 m from the walking level and the higher 1,10 m from the walking level.

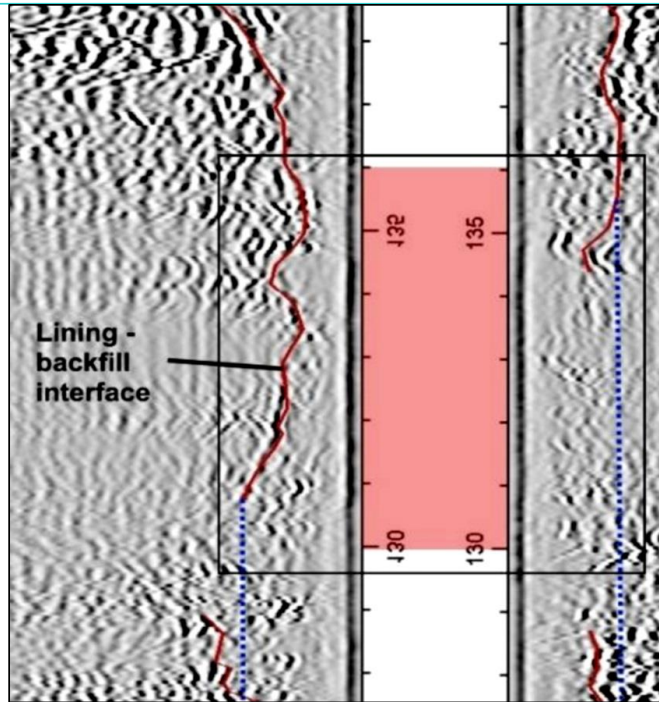


Fig. 14: Results of GPR. The red line represents the hewn stones – backfill interface.

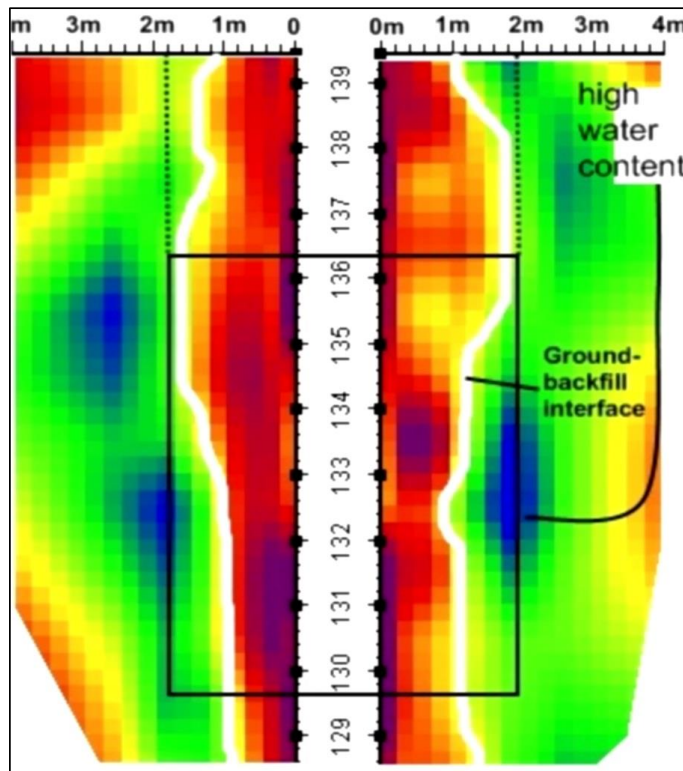


Fig. 15: Results of ERT 1,10 m above the walking level.

The pattern of the wall here is the same as the one described previously. The maximum wall thickness (solid rock blocks) is 50 cm, observed at **ch 0+131** at the west side. The ERT results are very striking. At level 1,10 m the excavation width (white line) is the maximum identified. It reaches 2 m on either side. Interesting is the fact that at level 0,60 m the excavation width reduces down to less than 1m. This can be explained by the presence of a cave-in (ground collapse) that occurred during excavation and enlarged both sidewalls. Areas of high water content are present on either side of the tunnel.

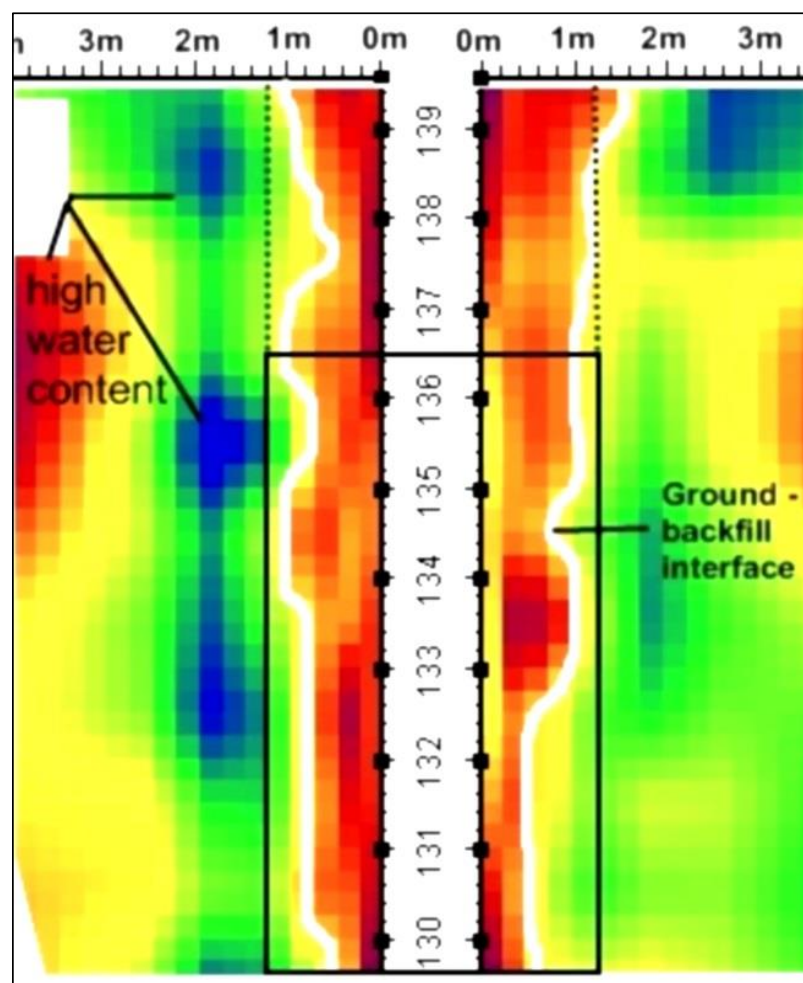


Fig. 16: Results of ERT at 0,60 m above the walking level.

This Roman type wall starts at **ch. 0+010**. It ends at **ch 0+050** ($l=40$ m). It is a mortared masonry wall of an arched shaped roof (Figure 17). The thickness of the mortared joints is 3 cm, the stone bricks are 3 to 15 cm thick and the roof arch is 25 to

35 cm high. The horizontal clearance of the lining is almost 0,60 m and the vertical is 1,60 m. This type of lining has also been constructed for 14,5 m from **ch. 0+ 205** to **0+219,50**.

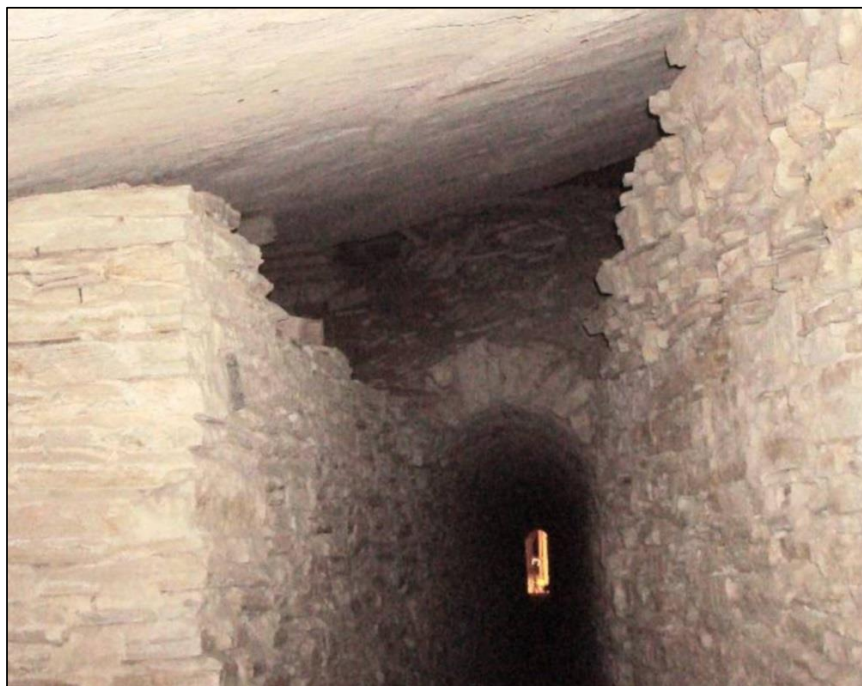


Fig. 17: Roman type wall of the north portal. The tunnel roof (geological bedding is subparallel to the tunnel axis) has collapsed on the arch of the wall. For a limited length the walls are vertical up to the tunnel roof.

The rock mass here consists of thinly bedded limestone with sub horizontal bedding. The excavation geometry above the lining is visible from **ch 0+011** (Figure 17). The tunnel roof has been gradually collapsing. Most likely this explains why this section was protected in the Roman era. Today, the arched roof is loaded with the weight of the debris that has fallen on it; when this weight became excessive the roof subsided and slipped (Figure 18).

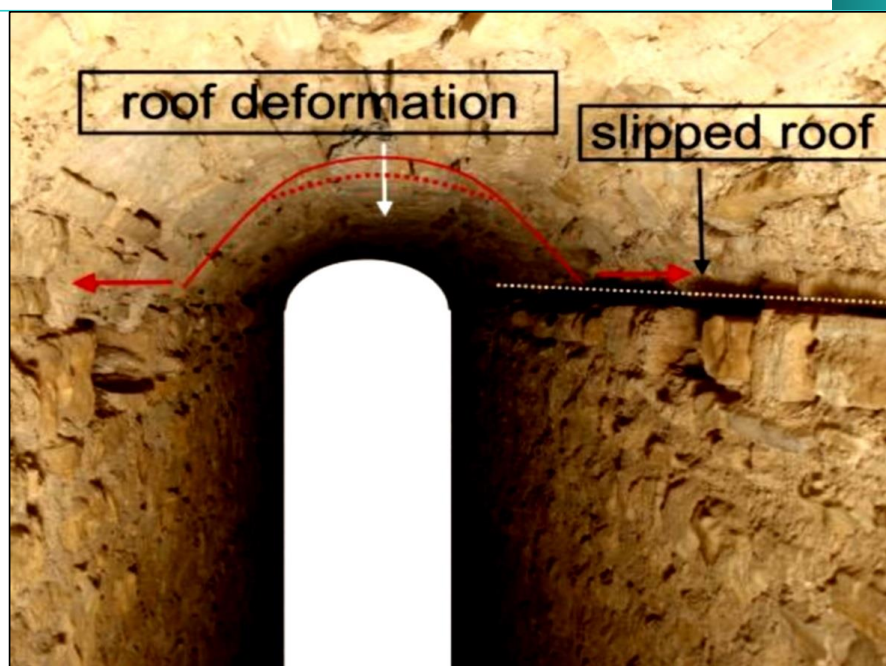


Fig. 18: Arched roof slipped and deformed

Here, the thicknesses measured by GPR are in good agreement with the actual width (25 to 30 cm) of the stones of the masonry wall. On the other hand the measured ERT thickness at the opposite sidewall is in good agreement with the sum of the actual thickness of the lining plus the thickness of the possible backfill.

3.2 Seismic refraction, VLF, SP, and ERT

The geophysical methods that have also been used along the walled tunnel section at the north bore involve surface to tunnel electrical resistivity tomography, seismic refraction, VLF (Very Low Frequency) and SP (Spontaneous Polarization) methods (Tsokas et al, 2014). The scope of these methods was to investigate the ground conditions of the tunnel's overburden. This is the ground between the tunnel crown and the surface. Figure 19 is a combined geological/geophysical longitudinal section along the north tunnel section that is protected by the dry masonry walls. The tunnel is shown by the green lines of the level +55. The locations where the wall has been damaged are marked by the black circles 1 to 6 on the tunnel. The black and the red lines are seismic and geoelectrical discontinuities respectively and have been recognized as fault zones. The grey and blue sections are areas of low velocity and resistance respectively and have been evaluated as areas of lower strength ground.

Along this tunnel section, surface geological mapping (Lyberis et al, 2013) has identified alternations of thinly bedded marls, green schistose clays and limestones. Many intersecting faults have been identified from **ch 0+090** to **ch 0+140**. Two major fault zones at **ch 0+220** and **ch 0+270** have been mapped as well.

The evaluated geophysical results are in good agreement with those of the geological mapping. The geophysical methods have identified the distribution of the major fault zones in the ground. They have also supplemented the geological mapping observations at the level of the tunnel, by recognizing, the areas of a poor/low strength ground adjacent to the faults. For example, the area of the intersecting faults from **ch 0+090** to **0+140** that was identified with the geological mapping at the surface was also identified (as a low resistance area) at the tunnel levels by the geophysical methods. It is of great interest that the damages identified at the tunnel masonry walls are located at the intersections of the tunnel with the fault zones mentioned earlier. Most of them occurred between **ch 0+090** to **0+140**. For example, a serious damage at the wall (Figure 20) at chainage **0+180** is located at the intersection with a major fault zone.

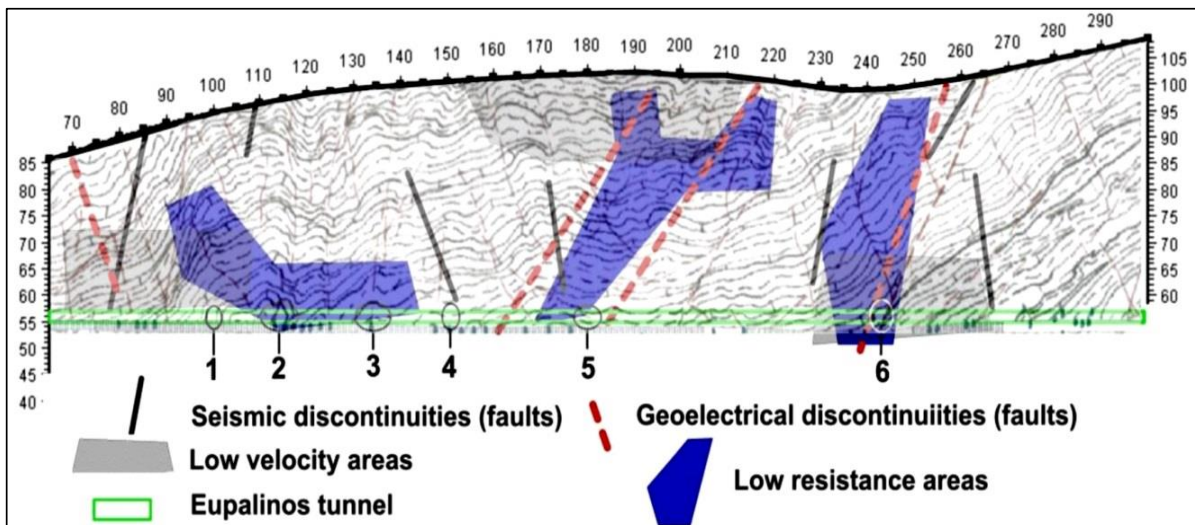


Fig. 19: Geophysical and geological longitudinal section along the lined (protected) tunnel section at the north bore (Tsokas et al, 2014). Damage on the wall: **1:0+100**, **2:0+110-0+117**, **3:0+130-0+136**, **4:0+149**, **5:0+178-0+184**, **6:0+245**.



Fig. 20: Fractured and displaced arched stones at chainage 0+180.

3.3 Ground geotechnical properties

As mentioned in the previous paragraph, the ground behind the walls comprises thinly bedded marls and green schistose clays. These (when sheared and faulted) form an amorphous soft clayey matrix with rock fragments (Figures 21 and 22).



Fig. 21: Thinly bedded marls, green schistose clays (some slippage of rock material has occurred along a planar joint to the right).



Fig. 22: Amorphous soft clayey matrix with rock fragments near the start of the first part of the Archaic wall.

To investigate the ground properties, soil samples were selected from an unprotected section (from **ch 0+204** and **0+235**) of the tunnel between two wall-protected tunnel sections. Tables 1 and 2 show laboratory test results of three soil samples selected. In two samples of remolded clay, the shear strength parameters were estimated after direct shearing. The residual angle of shearing resistance ϕ^0 was found equal to $27,1^\circ$ and $28,3^\circ$. The respective cohesion was found equal to 0 and 5,2 kPa respectively.

Sample	Description	Clay/Silt %	Sand %			Gravel %		Classif. U.S.C.S
			Fine	Medium	Coarse	Fine	Coarse	
204	Weathered marl-clay	77,6	7,6	5,9	3,7	5,2	0	CL
235a	Weathered marl-clay	72,6	10,9	8,8	3,6	4,1	0	CL
235b	Clay schist	49,2	1,9	3,4	5,7	9,6	30,2	SC

Table 1. Grain size distribution

Sample	Water content (%)	W _L (%)	W _P (%)	PI=W _L -W _P	Specific gravity
204	23,8	44,4	16,6	27,8	2,62
235a	28,5	44,3	16	28,3	2,56
235b	30,3	62	17	45	

Table 2. Atterberg limits and specific gravity

4. Methods and results of wall finite element analyses

4.1 Simplified analysis at ch 0+63,9

Considering also the results of the previous investigations, a simplified analysis was carried out in order to investigate the minor on-going fracturing (spalling) occurring at the front view of the Archaic wall at ch 0+63,9. This analysis was performed using the finite element code Phase 2 (www.rocscience.com). At this point, the wall has to bear the increasing weight of the gradually loosening rock mass. Loosening of the ground is a time dependent process that happens due to the deterioration of the ground (as it is exposed to variations in moisture, drying, temperatures). When the stresses induced in the stone blocks of the wall exceed their strength, the latter gradually fail (spalling). This process is illustrated in Figure 23.

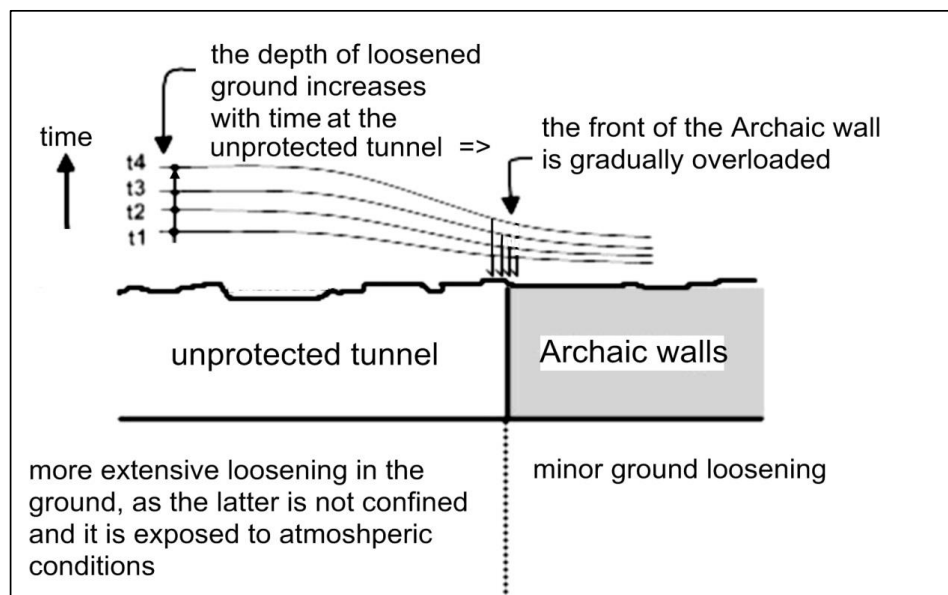


Fig. 23: Longitudinal section of the tunnel. Hypothesis to explain the minor failures (spalling) of the Archaic wall front.

The possible stress – strain distribution of the stone blocks of the roof has been investigated with the use of a simplified stress analysis. The strength parameters selected for the stone are 1,0 GPa for the modulus of elasticity, 3,0 MPa for the cohesion and 45° for the angle of shear resistance. An axisymmetric trapezoidal load distribution was applied to the top edge of the stone. The larger load (75 KPa) is at the side of the stone towards the unprotected tunnel section. The smaller load (50 KPa) is

towards the walled tunnel section (see Figure 8). At the top edge of the stones and due to the frictional forces between the first and the ground, only vertical movement was allowed in the modeling. The vertical movement was allowed at the vertical edge of the stone. The base of the stone was assumed to be fixed. Figure 24 shows the shear strain distribution of the stone. The hot colors represent areas of higher strain. The white circles are points within the stone, where tension failure occurs. The strain distribution and the shape of the area that fails in tension can explain the spalling observed (Figure 8).

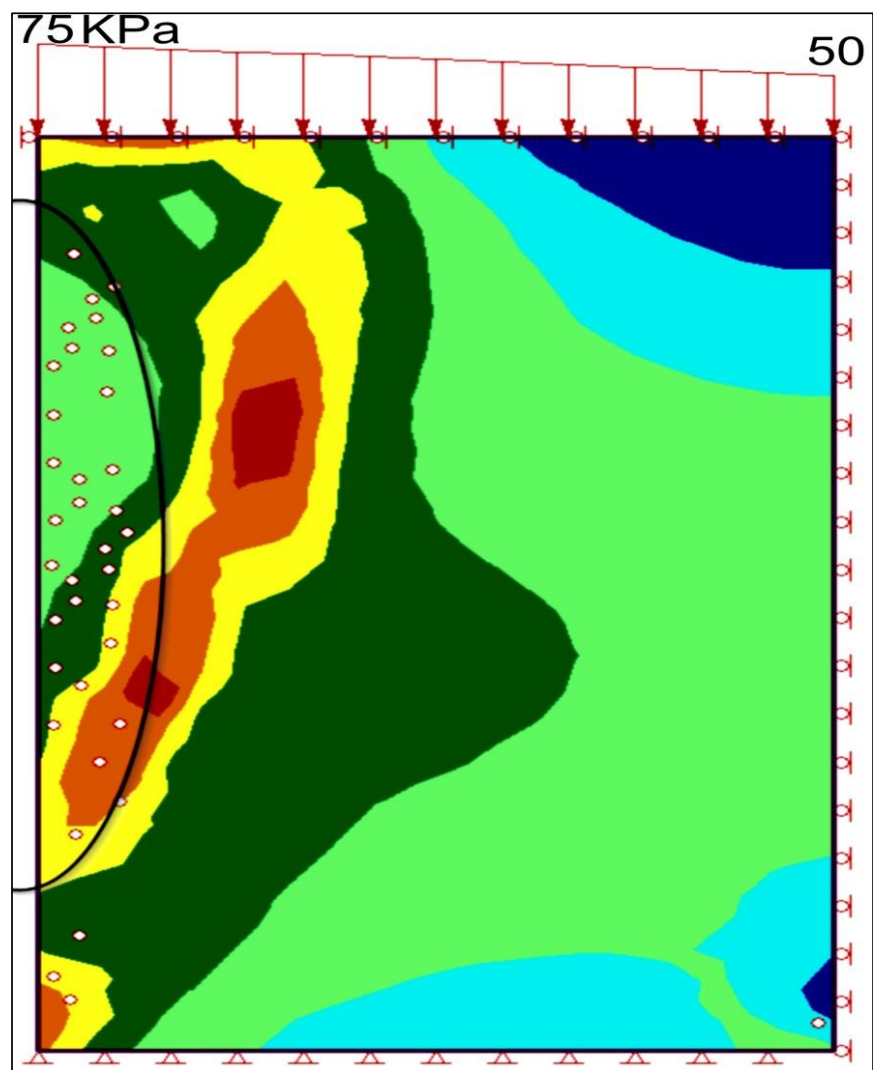


Fig. 24: Finite element analysis results. Shear strain distribution in the hewn stone.

4.2 Simplified analysis at ch 0+130

A simplified finite element analysis was also carried out in order to understand the failure pattern of the wall's roof of chainage **0+130** (Figure 13). The west stone block is significantly dislocated and is temporarily supported by a wooden wedge. The ground is simulated as a homogenous material with low strength properties. The pattern of the calculated deformation is shown in Figure 25. The deformation magnitude is similar to both sides of the wall (the maximum measured deformation is 5 cm).

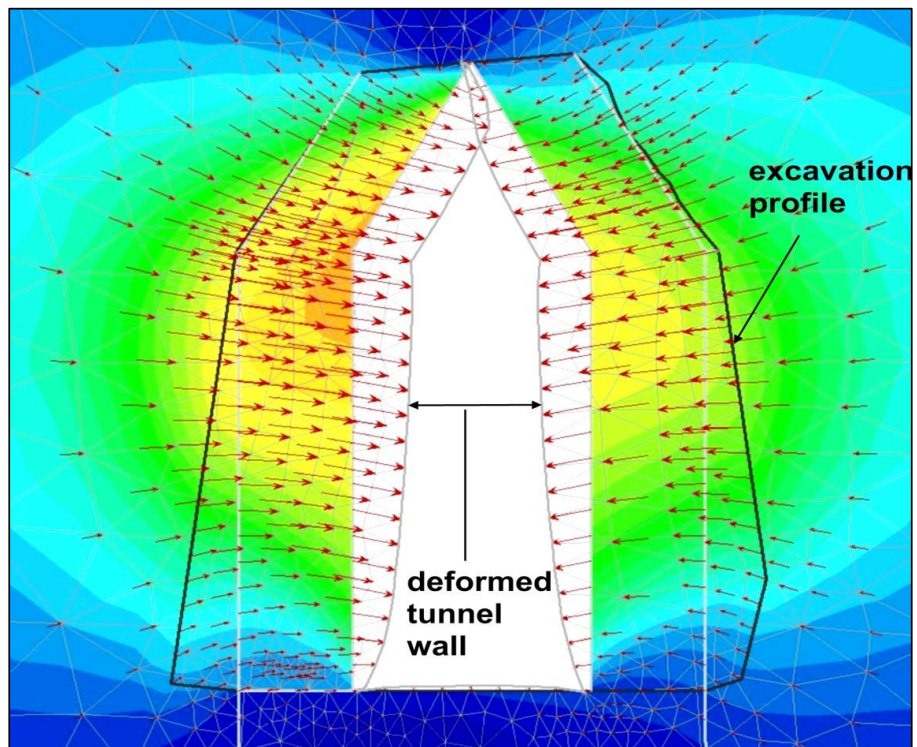


Fig. 25: Finite element analysis results. Deformation analysis of the wall at ch. 0+130.

However, the wall's deformation pattern changes significantly after the measured rock discontinuities are introduced into the ground model (Figure 26).

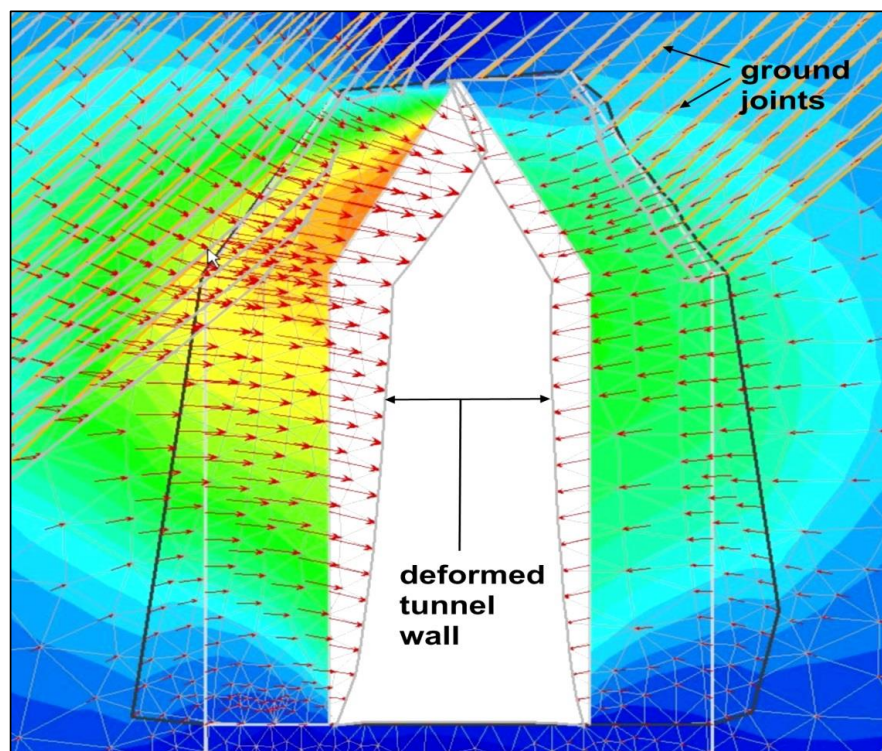


Fig. 26: Finite element analysis results. Deformation analysis of the wall at ch. 0+130. Joints have been introduced in the ground.

In this case, despite the fact that the deformation of the east wall remains the same, the deformation of the west wall is doubled; this explains both the real wall condition and to a certain extent the magnitude of the real deformation. The results of this simplified analysis show the possible impact the orientation of the joints in the ground may have on the failure pattern of the wall. It is impossible to estimate the time this damage occurred or what has been its real mechanism. It is most likely that the ground load was imposed gradually on the wall. Creep in the ground, excessive water pressures, swelling pressures due to minerals at fault gauge, seismic shocks, may have all contributed to some degree to the wall failure. In addition, when the contact of the two stone blocks of the roof was eventually lost, the stones slipped inwards. Then the ground behind the stone blocks was further relaxed and loosened and additional loads were imposed on the wall.

5. Methodology of the restoration works

The measures and the methodology selected to protect and restore the ancient walls, *mutatis – mutandis*, comply with those of the modern conventional tunnelling: The tunnel excavation is supported by steel sets, shotcrete and rockbolts. The final protection layer is placed afterwards. The arrangement and the properties of those measures are dependent on the ground properties.

The protection/restoration measures (Figure 27) that were dimensioned for the Archaic wall in brief include: a) staged dismantling of the wall piece by piece, b) supporting the ground behind the wall using stainless steel rock bolts, steel sets and a concrete mantle, c) rebuilding the wall to its original non-deformed position. These measures (steel sets, concrete mantle and rock bolts) aim to undertake the full ground loads so that the rebuilt wall will be practically unstressed.

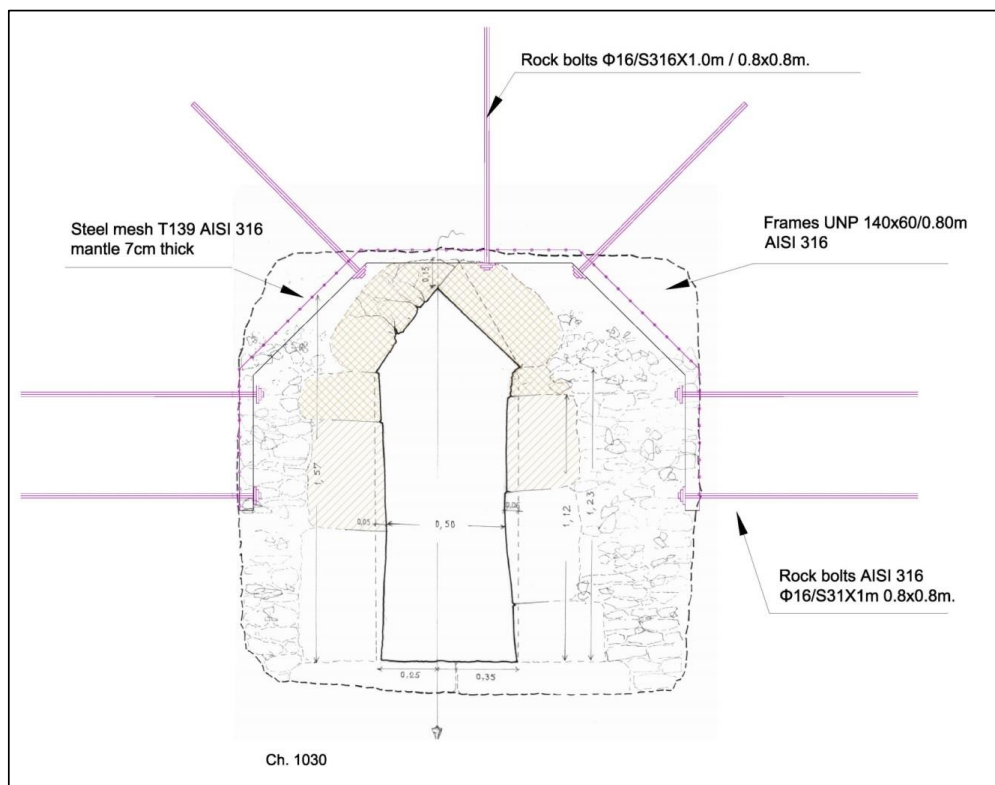


Fig. 27: Restoration measures at the Archaic wall. **1:** Staged dismantling of the wall, **2:** Stainless steel sets, **3:** Stainless steel rock bolts, **4:** Concrete mantle.

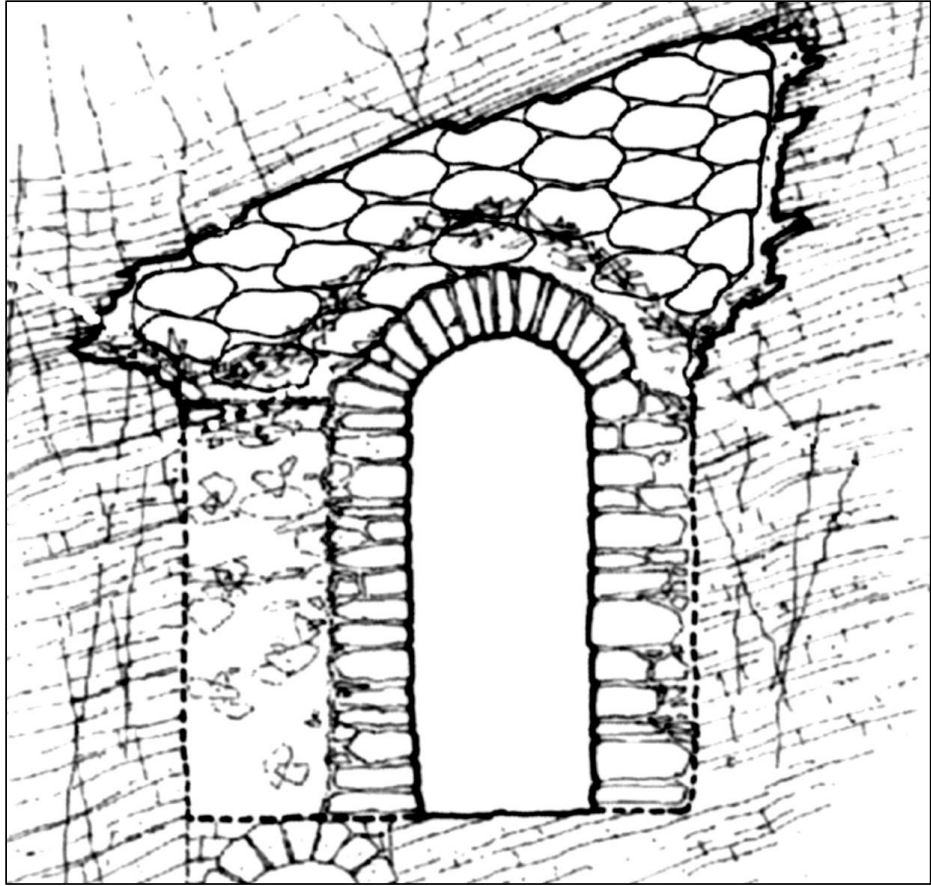


Fig. 28: Restoration measures. Roman wall.

For the Roman-type wall, the first measure proposed is the careful removal of the failed rock material accumulated above its arch. Where the height of the “cave-in” (ground collapse) is small, the space between the arch and the cave-in’s perimeter is proposed to fill with bags filled with lightweight material (Figure 28). The latter is proposed in order to avoid further rock falls from the tunnel roof.

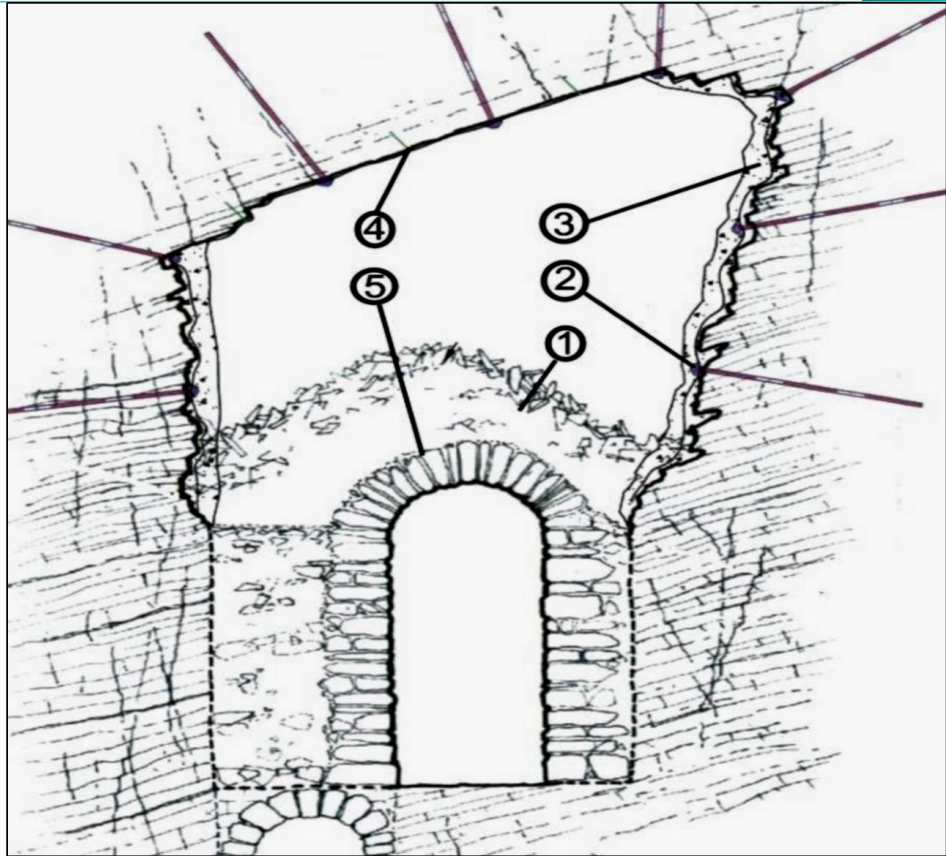


Fig. 29: Restoration measures at a large cave-in. Roman wall. **1:** Removal of debris, **2:** Stainless steel rock bolts, **3:** Concrete mantle, **4:** Short stainless steel nails and net, **5:** Arch strengthening

Stainless steel rock bolts combined with a concrete mantle are proposed to be installed at tunnel wall collapses of large dimensions. The latter in order to avoid further ground deterioration and subsequent rock falls (Figure 29). Works also include the removal of the failed ground material (debris) and the strengthening of the Roman-era wall using neutral grouts. In both cases the concept behind the restoration measures was to relieve and/or remove the ground loads that act on the walls, thus leaving them unstressed.

6. Discussion

Frequent ground collapses (cave-ins) would justify the Eupalinos' decision to protect the tunnel's excavation at certain sections. In the case of poor ground conditions that are associated with the presence of ground water, further ground collapses are expected. Such collapses also led to the construction of the Roman-type walls hundreds of years later. The ERT results on the tunnel masonry walls shed some light on the geometry of the tunnel excavation behind them. As shown in chapter 3, the ERT method identifies better the excavation boundary of the tunnel (or the backfill – ground interface). Figure 30 presents the ERT profile of the west wall, 1.10 m above the walking level of the tunnel, from chainage **0+065** to **0+087**. The predicted profile of the excavation – backfill boundary is depicted by the black line. The maximum distance of the black line from the line that represents the tunnel's wall is almost 2 m at chainage **0+077** and the minimum one is almost 0.5 m at chainage **0+070**. It is obvious that the assumed excavation profile is very irregular. The irregularity of the tunnel's excavation geometry can be most likely explained by assuming that the tunnel suffered many ground collapses there. Such ground collapses have also occurred along the unprotected section of the tunnel, in areas of unfavorable ground conditions. For example, Figure 31 shows a similar ground collapse at chainage **0+235**, which is between two wall-protected tunnel sections. Unfavorable ground conditions that could lead to a ground collapse include the adverse orientation of the bedding planes, low strength ground at fault zones and high groundwater pressures. The last is obvious nowadays, along the wall protected section of the tunnel. The first has been discussed in chapter 3.

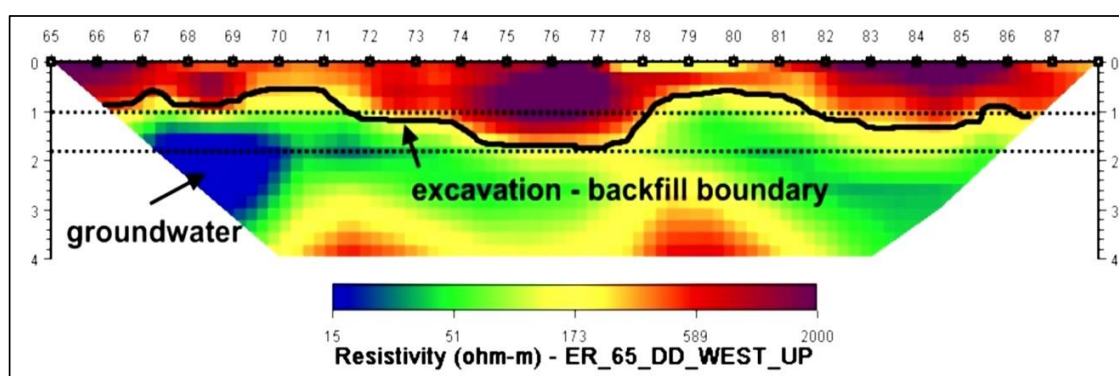


Fig. 30: Variation of the west side excavation geometry along a line located 1,10 m above the walking level. The maximum excavation width is almost 2 m at the west side. The lower is almost 0,6 m.



Fig. 31: Ground collapse $>1,5$ m located between the Archaic wall sections from 0+230 – 0+240.

7. Conclusions

The GPR method was found to predict well the wall–backfill interface or, in other words, the thickness of the wall's hewn stones. This was verified in all cases where the thickness of the hewn stones could be actually measured. On the other hand, the ERT method is able to predict the ground – backfill interfaces or in other words the sum of the thickness of the wall's hewn stones plus the thickness of the backfill material. The latter are the material between the wall hewn stones and the ground excavation perimeter. The results of these investigations were valuable in selecting and dimensioning the protection and restoration measures of the masonry walls.

The rest of the geophysical methods (seismic refraction, VLF, SP, and ERT) investigated the tunnel's overburden ground. In principal, their results explained to a certain extent the damages observed at the tunnel's walls. The damages to the walls

are located at the intersections of the tunnel with the fault zones and at a section of very poor/low strength ground as identified from geophysical investigation.

The restoration/protection measures of the masonry walls were selected to cope with the identified poor ground conditions. These measures (stainless steel sets, concrete mantle and stainless rock bolts) aim to undertake the full ground loads. Eventually the wall when rebuilt will practically carry no loads.

8. Acknowledgements & Closing Information

The design works of the aqueduct commenced in 2009, following the approval by the Ministry of Culture of Greece, financed by the Ministry of Public Works. The architectural design was carried out by Dr.Ing. Costas Zambas & Associates⁶. The restoration designs were jointly carried out by Dr.Ing. Costas Zambas and the geotechnical firm EDAFOS S.A. On behalf of EDAFOS S.A.⁷. Dr.Ing. George Dounias coordinated the geotechnical designs. The surveying works were carried out by Ing. Panagiotis Tokmakidis⁸ in cooperation with Prof. Kostas Tokmakidis⁹ of Aristotle University of Thessaloniki. The geophysical investigation was carried out by the Geophysical Laboratory of Aristotle University of Thessaloniki, co-ordinated by Prof. Grigoris Tsokas¹⁰. The electrical and mechanical designs were carried out by the design firm Vassilios Konstandinidis & Associates¹¹. Design works lasted almost 1½ years. All works were carried out in close cooperation along the help of the chief archaeologist of Samos Mrs. Maria Viglaki and the prefect of Samos Dr. Med. Manolis Karlas. The construction works are in progress by the construction company Edratec S.A. of Edrasis Group¹² and are expected to be completed by mid-2016.

9. References

Angistalis, George and Kouroumli Arend, Ourania, 2013. Outline of the Restoration Designs of Eupalinos Tunnel, Samos Island, Greece. In proceedings: 2nd Eastern European Tunnelling Conference Athens, Greece. Tunnelling in a Challenging Environment, 28 September - 01 October 2014. Greek Tunnelling Society.

Kienast Hermann, 1995. Die Wasserleitung des Eupalinos auf Samos (Samos XIX.). Deutsches Archailogical Institute. In Kommission Bei. Dr. Rudolph Habelt GMBH. Bonn. ISBN 3-7749-2713-8.

Lyberis, Evrikos, Ntouroupi, Anastasia, Sotiropoulos, Leonidas, Angistalis, Georgios, Dounias, Georgios, 2013. The geology of Eupalinos Aqueduct, Samos Island, Greece. In proceedings: 2nd Eastern European Tunnelling Conference Athens, Greece Tunnelling in a Challenging Environment, 28 September - 01 October 2014. Greek Tunnelling Society.

Stamatakis, Michalis, 1990. Building stones from the ancient quarries of Agiades area, Samos Island, Greece. In Proceedings: The engineering geology ancient works, monuments and historical sites (Preservation and Protection) Edited by Marinos P. and Koukis G., Volume 4, pages 2043-2047, Balkema, Rotterdam.

Tsokas, Gregory, Jung-Ho Kim, Tsourlos, Panagiotis, Angistalis, Georgios, Vargemezis, Georgios, Stampolidis, Alexandros, Diamanti, Nectaria, 2014. Investigating behind the lining of the Tunnel of Eupalinus in Samos (Greece) using ERT and GPR. Near Surface Geophysics. EAGE. DOI: 10.3997/1873-0604.2015012. Special topic: Integrated Geophysical Investigations for Archaeology.

Tsokas, Gregory, Tsourlos, Panagiotis, Jung-Ho Kim, Papazachos, Constantinos, Vargemezis, George, Bogiatzis, Petros, 2014. Assessing the Condition of the Rock Mass over the Tunnel of Eupalinus in Samos (Greece) using both Conventional Geophysical Methods and Surface to Tunnel Electrical Resistivity Tomography. Archaeological Prospection. Volume 21, Issue 4, pages 277–291, October/December 2014.

¹ The authors' names are in alphabetical order.

² Egnatia Odos S.A. is a state-owned company, responsible for the design and construction of the Egnatia Odos Motorway, a 680 km project (and its vertical axes leading to the Balkan Peninsula), in northern Greece. The length of the operating tunnels along the Egnatia Motorway is almost 100 km.

³ Hermann J Kienast: Die Wasserleitung des Eupalinos auf Samos (Samos XIX.), Rudolph Habelt, Bonn 1995. ISBN 3-7749-2713-8.

⁴ The aqueduct of Eupalinos in Samos. Herman Kienast. Ministry of Culture. Archaeological Receipts Fund, 2004, ISBN 960-214-368-1, ISBN-13 978-960-214-368-1, 58 pgs. Translation: Konstantinos Tsakos.

⁵ The ruler of Samos Kostakis Adosidis formed a committee responsible for the organization and supervision of the works. The monks Theofanis Arelis and Kyrillos

Moninas from the monastery of the “Holy Cross “have been the persons responsible for the supervision of the works.

⁶ Costas Zambas, Dr. Civil Engineer, Skiathou 43-11254, Athens, Greece, 210 2237167, c-zambas@hol.gr, Associates: Gerasimos Thomas Dr. Civil Engineer, Eirini Doudoumi, Architect MSc

⁷ Edafos Consulting Engineers S.A. Iperidou 9, 10558, Athens, Greece, 210-3222050, admin@edafos.gr

⁸ Panagiotis Tokmakidis, Dimokritou 32, 55132 Kalamaria, Thessaloniki, 2310996107, ktok@auth.gr

⁹ Prof Kostas Tokmakidis, AUTH, Dept Geodesy & Topography, Univer P.O. Box 432, 2310 996107, -//-

¹⁰ Prof Grigorios Tsokas, AUTH, Dept of Geophysics, 2310 998507, gtsokas@geo.auth.gr

¹¹ V. Konstantinides & Associates Ltd, Varnali 8, 543 52 Thessaloniki, Greece, 2310 929951, basicon@otenet.gr

¹² 47th km. of Attiki Odos, P.C. 19 400, KOROPI, Tel.: (+30) 210 66 80 600, edraasis@edraasis.gr